

# Synthesis of Mesoporous Amorphous Silica via Silica-Polyviologen Hybrids Prepared by the Sol–Gel Route

Michael J. Adeogun and John N. Hay\*

Department of Chemistry, School of Physics & Chemistry, University of Surrey, Guildford, Surrey, GU2 5XH, England

Received August 24, 1999. Revised Manuscript Received November 15, 1999

A range of polyviologens synthesized by the Menshutkin reaction have been successfully incorporated into silica hybrids using the hydrolytic sol–gel route. Transparent hybrids can be obtained with up to 75% polyviologen content, indicating a likely nanoscale morphology. Hybrids were calcined at 650 °C to remove the polymer, forming porous amorphous silica products. Nitrogen adsorption–desorption studies have been undertaken on the hybrids and the calcination products, and the results are analyzed by the modeless method of Brunauer et al. for mesopore size distributions and a micropore analysis method based on t-curves. The hybrids are mostly mesoporous solids, but porosities are very low at high polymer contents. Calcination leads to silicas which are mainly mesoporous with varying degrees of microporosity depending on the nature and concentration of the polyviologen (PV) used. Poly(hexyl viologen ditosylate) produces high surface area silicas with >98% mesoporosity. The results may provide evidence for an influence of the PV on the structure of the forming silica, which is proposed to occur through electrostatic interactions between the quaternary nitrogen atoms of the polymer and the silanol oxygen atoms in the growing silica network.

## Introduction

The synthesis of silica with controlled porosity has attracted considerable interest in recent years because of the range of potential applications for the products, including their use in catalysis and as catalyst supports, in separation processes and in sensors. One route to producing this porosity has been the use of small molecules or polymers incorporated into the forming silica network as structure control agents which are subsequently removed to leave the desired porosity. Structure direction is well-known in the field of zeolite chemistry, in which organic species are used to synthesize zeolites with specific pore sizes and shapes.<sup>1</sup> For example, the tetrapropylammonium ion acts as a structure directing agent for the synthesis of the pure silica zeolite, Si-ZSM-5.<sup>1,2</sup> Recent work has helped to establish the detailed mechanisms responsible for the development of the structure of these crystalline solids.<sup>1–3</sup>

A variety of templates have been studied for the control of porosity in amorphous silica synthesized by the hydrolytic sol–gel route. In templating, the network structure forms in such a way that removal of the template in principle creates a cavity with morphological and/or stereochemical features related to those of the template, including the size and shape of the template. In practice, this depends on factors such as the nature of the interactions between the template and

the matrix, the ability of the matrix to conform to the template, and possible matrix restructuring during template removal, which is often achieved by thermal degradation of the organic template. Two types of templates have in general been used, covalently bonded and nonbonded systems.<sup>4</sup> The latter includes small molecules, polymers, supramolecular arrays<sup>5</sup> and even bacteria,<sup>6</sup> which can template the growth of inorganic species via electrostatic, van der Waals, and hydrogen-bonding interactions, or combinations thereof. For example, in mesoporous silica synthesis using charged surfactant templates, electrostatic interactions are believed to play a key role in the initial organization of the organic–surfactant array.<sup>5</sup> Covalently bonded organic templates are those in which an organic moiety is covalently bonded to the silica precursor and are thus present in the initial organic–inorganic hybrid product,<sup>7,8</sup> which can then be thermally decomposed to the desired silica product. Corriu et al.<sup>9</sup> have recently described an approach based on chemical cleavage of the silica–organic bond which can potentially overcome the drawback of thermal reorganization of the inorganic network, although careful selection of the reagents is required to avoid a chemical rearrangement.

(4) Raman, N. K.; Anderson, M. T.; Brinker. C. J. *Chem. Mater.* **1996**, *8*, 1682.

(5) Dabadie, T.; Ayrat, A.; Guizard, C.; Cot, L.; Robert, J. C.; Poncelet, O. *Mater. Res. Soc. Symp. Proc.* **1994**, *346*, 849.

(6) Davis, S. A.; Burkett, S. L.; Mendelson, N. H.; Mann, S. *Nature* **1997**, *385*, 420.

(7) Hay, J.; Porter, D.; Raval, H. *Chem. Commun.* **1999**, 81.

(8) Ou, D. L.; Seddon, A. B. *J. Non-Cryst. Solids* **1997**, *210*, 187.

(9) Bours, B.; Chevalier, P.; Corriu, R. J. P.; Delord, P.; Moreau, J. E.; Chiman, M. W. *Chem. Mater.* **1999**, *11*, 281.

(1) Helmkamp, M. M.; Davis, M. E. *Annu. Rev. Mater. Sci.* **1995**, *25*, 161.

(2) Burkett, S. L.; Davis, M. E. *Chem. Mater.* **1995**, *7*, 1453.

(3) Davis, M. E.; Chen, C.-T.; Burkett, S. L.; Lobo, R. F. *Mater. Res. Soc. Symp. Proc.* **1994**, *346*, 831.

Both polymers and oligomers have been used to synthesize a wide range of organic–inorganic hybrids by the hydrolytic sol–gel route and the polymeric species or their supramolecular assemblies can act as templates for the resulting silica structure.<sup>10,11</sup> Cationic polymers have been little studied for this purpose,<sup>11</sup> despite the fact that cations and cationic surfactant assemblies are used to form porous crystalline zeolites and amorphous mesoporous silicas. In addition, there is clear evidence of the importance of functionality in controlling the structure of natural organic–inorganic hybrid materials,<sup>6,12</sup> and so it might be envisaged that synthetic charged polymers could exert a structure directing effect on sol–gel silica synthesized in their presence. We have previously reported the synthesis and characterization of a range of novel silica hybrids based on bipyridinium cationic ionene polymers (“polyviologens”).<sup>13</sup> Subsequent studies using small-angle X-ray scattering (SAXS) have also illustrated a likely structure-directing effect of the polyviologens during the sol–gel silica synthesis which can lead to the formation of products where the silica demonstrates an unusual surface fractal geometry,<sup>14</sup> in contrast to the mass fractal normally observed as a result of the acid-catalyzed sol–gel process. The aim of the work reported here is to study the effect of polyviologen incorporation on the pore structure of the sol–gel hybrid products and the resultant silica networks obtained by calcining the hybrids to remove the organic polymer. Detailed nitrogen adsorption–desorption studies were undertaken to assess this effect.

### Experimental Section

**Chemicals.** Reagents used were standard laboratory or AR grades which were used as received, unless stated otherwise below. Chemicals used were 4,4'-dipyridyl (98%, Lancaster; Avocado),  $\alpha,\alpha'$ -dibromo-*p*-xylene (97%, Aldrich), 1,4-dibromobutane (99%, Lancaster), 1,6-hexanediol (99%, Avocado), 1,4-butanediol (99%, Avocado), *p*-toluenesulfonyl chloride (98%, Aldrich), ethyl acetate (HPLC grade, Fischer), tetraethoxysilane (98+%, Lancaster), tetramethoxysilane (98%, Aldrich), methanol (HPLC grade, Fischer), absolute alcohol 100 (HPLC grade, Sigma-Aldrich), and glacial acetic acid (AR grade, Fischer). Acetonitrile (HPLC grade, Fischer) was dried over 3 Å molecular sieves and distilled before use.

**Instrumentation.** Infrared (IR) spectra of the polyviologens and the sol–gel hybrids were recorded on a Perkin-Elmer 1750 Fourier transform IR (FT-IR) spectrometer. Polyviologens and silica–polyviologen hybrids were prepared as KBr disks. (Spectroscopic grade potassium bromide (Sigma) was predried at 100 °C overnight.)

<sup>1</sup>H nuclear magnetic resonance (NMR) spectra were obtained using a Bruker AC-300 NMR spectrometer operating at 300.15 MHz. For the polyviologens, either D<sub>2</sub>O (deuterated water) or CD<sub>3</sub>OD (deuterated methanol) was used as the solvent. The number of scans performed was 16 with an acquisition time of 1.819 s.

Ultraviolet/visible (UV/vis) spectra of the polyviologens were obtained using a Philips PU 8720 UV/vis scanning spectrometer. Solutions of the polyviologens were prepared by dissolving the polymer in either distilled water or methanol.

Analyses for carbon, hydrogen, and nitrogen were carried out on an Exeter Analytical EA440 machine.

Uncorrected melting points were determined using a Gallenkamp melting point instrument.

Polymer light microscopy (PLM) studies were performed on a Zeiss D-7082 AXIOPHOT photomicroscope equipped with cross-polarizers and using transmitted light. A number of polyviologen solutions were prepared with varying concentrations either by dissolving a known amount of polyviologen in a known amount of distilled water and then evaporating off a certain amount of water by heating at ~90 °C, or by the simple dissolution of the polyviologen in a known amount of distilled water or methanol. Silica–polyviologen sol–gel solutions were also studied. Liquid films were prepared by adding three drops of the polymer or sol–gel solution to a microscope slide.

N<sub>2</sub> adsorption–desorption isotherms at 77 K were obtained using a Coulter SA 3100 surface area analyzer. After gelation, the sol–gel glasses were left at room temperature for 2 days, followed by a thermal treatment of 10 days at 80 °C. The samples were then outgassed for 10 h at 110 °C before analysis. Analysis of the surface area and porosity of the hybrids and the silica products resulting from calcination was based on the method derived by Brunauer, Emmett, and Teller (BET).<sup>15,16</sup> The method selected for determining pore size distributions for the silica–PV hybrids was the modeless method of Brunauer et al.,<sup>17</sup> which assumes no shape for the pores. The method utilizes the Kiselev equation for determining the core surface area of a group of pores. In this study, uncorrected data have been used since they give a reasonable representation of all core properties of interest, the calculations are simple, and the calculated properties are valid for cores of any shape. When there has been evidence of microporosity, correction terms and a cylindrical model have been employed to obtain a complete pore size distribution curve.<sup>17,18</sup> The micropore analysis method<sup>19</sup> (MP method) used in this study is based on the Cranston–Inkley composite *t* curve.<sup>18</sup> The MP analysis method<sup>19</sup> has been used to obtain micropore size distributions only for those materials in which microporosity was observed when the Harkins Jura equation<sup>20</sup> (eq 1) was used to determine *t* values.

$$t = 3.54 [5/(2.303 \times \log P_0/P)]^{1/3} \quad (1)$$

The volume adsorbed data are plotted against the calculated film thickness. These *t* plot data are then used to calculate the *y* intercept value which when converted from a gas volume to a liquid volume gives the micropore volume.<sup>20</sup> The slope of the linear section is used to calculate the meso-/macropore surface area.<sup>20</sup>

$$\text{volume}_{\text{micropore}} = (0.001547)(t \text{ plot intercept}) \text{ cm}^3 \text{ g}^{-1} \quad (2)$$

$$\text{surface area}_{\text{mesopore}} = 1547(t \text{ plot slope}) \text{ m}^2 \text{ g}^{-1} \quad (3)$$

$$\text{surface area}_{\text{micropore}} = \text{surface area}_{\text{BET}} - \text{surface area}_{\text{mesopore}} \text{ m}^2 \text{ g}^{-1} \quad (4)$$

The Coulter 3100 surface area analyzer provides the isotherm

(10) Sommerdijk, N. A. J. M.; van Eck, E. R. H.; Wright, J. D. *Chem. Commun.* **1997**, 159.

(11) Sato, S.; Murakata, T.; Suzuki, T.; Ohgawara, T. *J. Mater. Sci.* **1990**, *25*, 4880.

(12) Heuer, A. H.; Fink, D. J.; Laraia, V. J.; Arias, J. L.; Calvert, P. D.; Kendall, K.; Messing, G. L.; Blackwell, J.; Rieke, P. C.; Thompson, D. H.; Wheeler, A. P.; Veis, A.; Caplan, A. I. *Science* **1992**, *255*, 1098.

(13) Adeogun, M. J.; Hay, J. N. *Polym. Int.* **1996**, *41*, 123.

(14) Adeogun, M. J.; Fairclough, J. P. A.; Hay, J. N.; Ryan, A. J. *J. Sol-Gel. Sci. Technol.* **1998**, *13*, 27.

(15) Gregg, S. J.; Sing, K. S. W. *Adsorption, Surface Area and Porosity*; Academic Press: London, 1967.

(16) Lowell, S.; Shields, J. E. *Powder Surface Area and Porosity*, 3rd ed.; Chapman and Hall: London, 1991.

(17) Brunauer, S.; Mikhail, R. SH.; Bodor, E. E. *J. Colloid Interface Sci.* **1967**, *24*, 451.

(18) Mikhail, R. SH.; Brunauer, S.; Bodor, E. E. *J. Colloid Interface Sci.* **1968**, *26*, 54.

(19) Mikhail, R. SH.; Brunauer, S.; Bodor, E. E. *J. Colloid Interface Sci.* **1968**, *26*, 45.

(20) *Coulter™ SA3100 Product Manual*; Coulter Corp.: Miami, FL, Aug 1996.

**Table 1. Elemental Analysis of the Polyviologens Containing Tosylate (TsO<sup>-</sup>) Counterions**

PV <sup>a</sup>	calculated/mass %	experimental/mass %	M <sub>n</sub>
PBV-OTs	calculated for C <sub>28</sub> H <sub>30</sub> N <sub>2</sub> O <sub>6</sub> S <sub>2</sub> : C, 60.61; H, 5.45; N, 5.05	found 1: C, 59.34; H, 5.47; N, 5.01 found 2: C, 59.22; H, 5.42; N, 5.05	6500
PHV-OTs	calculated for C <sub>30</sub> H <sub>34</sub> N <sub>2</sub> O <sub>6</sub> S <sub>2</sub> : C, 61.81; H, 5.88; N, 4.81	found 1: C, 61.09; H, 5.90; N, 5.21 found 2: C, 61.62; H, 6.00; N, 5.38	6566

<sup>a</sup> PV = polyviologen, PBV-OTs = Poly(butyl viologen ditosylate), PHV-OTs = Poly(hexyl viologen ditosylate).

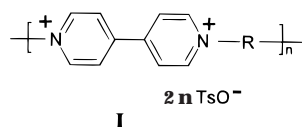
**Table 2. Selected IR and <sup>1</sup>H NMR Data for the Polyviologens Containing Tosylate (TsO<sup>-</sup>) Counterions**

PV	absorption maxima (cm <sup>-1</sup> )	corresponding functionality	chemical shift, δ (ppm) <sup>a</sup>	corresponding functionality
PBV-OTs	1639 (vs)	C=N stretch	4.72	<sup>+</sup> N-CH <sub>2</sub> -
	1497 (med) and 1599 (med)	C-C skeletal stretch	7.2-7.9	dd, 8H, ArH
	1122 (s) and 1359 (s)	-S=O stretch	8.6-9.3	dd, 8H, hetero ArH
	1192 (s)	C-N <sup>+</sup> stretch		
PHV-OTs	1640 (vs)	C=N stretch	4.85	<sup>+</sup> N-CH <sub>2</sub> -
	1495 (med) and 1597 (med)	C-C skeletal stretch	7.1-7.6	dd, 8H, ArH
	1125 (s) and 1339 (s)	-S=O stretch	8.4-9.3	m, 8H, hetero ArH
	1195 (s)	C-N <sup>+</sup> stretch		

<sup>a</sup> In CD<sub>3</sub>OD.

data, BET surface areas, BET constants (*C* values), total pore volumes, micropore volumes, and surface areas (eqs 2-4). By using the appropriate equations and *t* curves, the pore sizes of the silica-polyviologen sol-gel hybrids were then calculated.

**Polyviologen (PV) synthesis.** Polyviologens containing bromide counterions were synthesized as described in our earlier paper:<sup>13</sup>



Polyviologens containing tosylate counterions (e.g., **I**) were synthesized from the corresponding alkane ditosylates, which were synthesized according to literature methods.<sup>21</sup> 1,4-Butane ditosylate was obtained in 50% yield, mp 68-69 °C (lit.<sup>22</sup> 67.5-69.5 °C) and 1,6-hexane ditosylate in 68% yield, mp 70-72 °C (lit.<sup>23</sup> 71-72 °C). The synthesis of the polyviologens is illustrated by the preparation of poly(butyl viologen ditosylate), PBV-OTs:

4,4'-Dipyridyl (1.491 g, 9.55 mmol) and 1,4-butane ditosylate (3.960 g, 9.94 mmol) were reacted with stirring in dry acetonitrile (85 mL) at 82 °C for 120 h. During the polymerization reaction, a partial precipitation occurred. At the end of the reaction, the reaction flask was cooled to room temperature and the polymer was precipitated out completely with the addition of ethyl acetate (~250 mL). The polymer was filtered under suction and dried in vacuo at 80 °C for 24 h. An off-white powder was obtained (4.769 g; 90% yield).

Poly(hexyl viologen ditosylate), PHV-OTs, was obtained in a similar way in 90% yield. The polyviologens were analyzed in a similar way to previous work.<sup>13</sup> Elemental analyses for PBV-OTs and PHV-OTs are presented in Table 1, along with the calculated value for M<sub>n</sub>.

IR and <sup>1</sup>H NMR data for the tosylates are summarized in Table 2.

**Synthesis of Silica-Polyviologen Hybrids.** The hybrids were generally synthesized<sup>13</sup> by one of four methods depending on the nature and the amount of polyviologen incorporated. These methods are outlined below (although the amounts of reactants used differ depending on the hybrid system).

**Method 1.** PXV-Br (0.096 g, 2.3 mmol) was dissolved in distilled water (4.125 g, 229 mmol). To this solution was added

ethanol (absolute alcohol 100) (0.88 g, 19.1 mmol). The mixture was shaken to dissolve as much polymer as possible. Glacial acetic acid (0.581 g, 9.7 mmol) was then added, and upon addition all the polymer dissolved to give a yellow, transparent liquid. Tetraethoxysilane (TEOS) (3.998 g, 19.2 mmol) was added, and the resulting mixture became turbid. On standing, the mixture separated into two layers. The mixture was stirred vigorously until homogenization had taken place. The sample bottle was covered with perforated "Parafilm" to allow for solvent evaporation. After 2 days at room temperature, the mixture had gelled to give a yellow, transparent gel. The brittle solid was then dried at 80 °C for 72 h during which time the sample cracked catastrophically. The solid was then dried for a further 45 h at 120 °C to produce a yellow, transparent, glassy material.

**Method 2.** To an empty sample bottle was added PXV-Br (0.301 g, 0.72 mmol), followed by distilled water (15.003 g). The bottle was shaken to try to dissolve as much of the polymer as possible, and then stirred vigorously. The polymer solution was heated using a hot plate until the amount of water had been reduced significantly. After this heat treatment (~1 h) the amount of water had been reduced to 2.656 g (147 mmol). The clear yellow solution was allowed to cool slightly, and ethanol (0.503 g, 10.9 mmol), glacial acetic acid (0.576 g, 9.3 mmol) and TEOS (1.996 g, 9.6 mmol) were added. The liquid separated into two layers when left to stand and so the solution was stirred vigorously until homogeneous (~1 h). The sample bottle was covered with "Parafilm" (which was perforated to allow solvent evaporation) and left for 78 h at room temperature (gelation occurred after 22 h). After this time at room temperature some cracks had started to develop. The sample was placed in an oven at 80 °C for 2 weeks. After this heat treatment the sample had broken up considerably and a yellow/brown homogeneous, transparent, glassy product was obtained.

**Method 3.** This method was similar to that described in method 1, except the order of addition of the reactants was as follows: (1) PV; (2) methanol; (3) tetramethoxysilane (TMOS); (4) glacial acetic acid; (5) distilled water. Additionally, the samples were left at room temperature for ~72 h, followed by heat treatment at 80 °C for 10 days. The appearance of the glassy products is summarized in Table 3.

**Method 4.** This method was similar to that described in method 1, except the order of addition of the reactants was as follows: (1) PV; (2) distilled water; (3) TMOS; (4) methanol; (5) glacial acetic acid. Additionally, the samples were left at room temperature for ~72 h, followed by heat treatment at 80 °C for 10 days. The appearance of the glassy products is summarized in Table 3.

The hybrids synthesized and the reaction conditions used are summarized in Table 3.

(21) Johns, W. F.; Lukes, R. M.; Sarett L. H. *J. Am. Chem. Soc.* **1954**, *76*, 5026.

(22) Martin, A. E.; Ford, T. M.; Bulkowski J. E. *J. Org. Chem.* **1982**, *47*, 412.

(23) Fear, E. J.; Thrower, J.; Veitch, J. *J. Chem. Soc.* **1958**, 1322.

Table 3. Reaction Conditions Used for Hybrid Synthesis

PV used	wt % PV <sup>a</sup>	alkoxide	method	<i>r</i> <sup>e</sup>	<i>r</i> <sub>s</sub> <sup>f</sup>	<i>r</i> <sub>a</sub> <sup>g</sup>	pH <sup>h</sup>	gelation time/h	appearance
neat silica	0	TMOS	3 <sup>c</sup>	2.0	1.0	0.99	2.0	48	colorless; transparent
neat silica	0	TMOS	3 <sup>c</sup>	30.0	0.97	0.97	3.0	48–72	colorless; transparent
PBV–Br	1	TMOS	1 <sup>c</sup>	3.4	1.0	0.45	1.5	23	yellow; transparent
PBV–Br	10	TMOS	1 <sup>c</sup>	5.8	1.0	0.51	2.0	21	dark yellow; transparent
PBV–Br	20	TMOS	2 <sup>d</sup>	6.85	1.0	0.47	2.5	23	yellow/brown; transparent
PBV–OTs	30	TMOS	4 <sup>c</sup>	2.0	0.97	0.5	1.5	19	yellow; transparent
PBV–OTs	37	TMOS	4 <sup>c</sup>	2.0	0.97	0.5	2.0	19	yellow; transparent
PXV–Br	8	TEOS	1 <sup>d</sup>	11.6	0.99	0.48	3	50	orange; transparent
PXV–Br	10.5	TEOS	1 <sup>b</sup>	15.9	1.0	1.0	2.0	< 26	yellow; transparent
PXV–Br	53.8	TEOS	2 <sup>b</sup>	25.8	1.0	0.78	1.5	21	dark yellow; transparent
PHV–OTs	12.6	TMOS	3 <sup>c</sup>	26.5	0.2	0.99	2.0	22	yellow; transparent
PHV–OTs	29	TMOS	3 <sup>c</sup>	3.4	0.6	1.0	1.5	2	yellow; transparent
PHV–OTs	49	TMOS	3 <sup>c</sup>	4.9	4.9	1.0	3.0	48	dark yellow; translucent
PHV–OTs	75	TMOS	3 <sup>c</sup>	4.98	9.6	1.1	3.0	48	yellow/brown; transparent

<sup>a</sup> Assuming complete hydrolysis and condensation of the alkoxide precursor to SiO<sub>2</sub>. <sup>b</sup> Solvent = ethanol (absolute alcohol 100). <sup>c</sup> Solvent = methanol. <sup>d</sup> Solvent = *N,N*-dimethylformamide (DMF). <sup>e</sup> *r* = water:alkoxide molar ratio. <sup>f</sup> *r*<sub>s</sub> = solvent:alkoxide molar ratio. <sup>g</sup> *r*<sub>a</sub> = acid:alkoxide molar ratio. <sup>h</sup> pH estimated using pH paper.

Table 4. Surface Area Analysis of Silica and Silica–PV Hybrids

PV used <sup>a</sup>	% PV <sup>b</sup>	BET surface area/m <sup>2</sup> g <sup>-1</sup>	C value	total pore volume (V <sub>p</sub> ) <sup>c</sup> /cm <sup>3</sup> g <sup>-1</sup>	porosity (φ) <sup>d</sup> /%	average pore diameter (D) <sup>e</sup> /Å
silica ( <i>r</i> = 2)	0	702	436	0.349	43	17.9
silica ( <i>r</i> = 30)	0	690	242	0.353	44	18.4
PBV–Br	1	565	319	0.294	39	18.7
PBV–Br	10	474	76.2	0.283	38	21.5
PBV–Br <sup>f</sup>	20	1.02	40.0	0.0015	0.3	52.9
PBV–OTs <sup>f</sup>	30	0.406	24.5	0.0027	1	239
PXV–Br	8	365	66.1	0.287	39	28.3
PXV–Br	10.5	457	190	0.222	33	17.4
PXV–Br <sup>f</sup>	53.8	10.5	40.6	0.013	3	45.0
PHV–OTs <sup>f</sup>	12.6	432	49.4	0.316	41	26.3
PHV–OTs <sup>f</sup>	29	110	37.3	0.085	16	27.7

<sup>a</sup> See Table 3 for synthetic method. <sup>b</sup> PV = polyviologen. <sup>c</sup> At *P/P*<sub>0</sub> = 0.9907. <sup>d</sup> Porosity, φ = V<sub>p</sub>/(V<sub>p</sub> + 0.455)(100%). <sup>e</sup> Average pore diameter, D = 0.9(4V<sub>p</sub>/A); A is the BET specific surface area. <sup>f</sup> Synthesized from a lyotropic solution of polyviologen.

## Results and Discussion

**Synthesis of PVs and PV–Silica Hybrids.** The polyviologens were synthesized according to methods described previously<sup>13</sup> starting from dibromoalkanes or alkane ditosylates. The ditosylate-containing polymers were generally obtained in higher yields than those derived from the corresponding dibromoalkanes, reflecting the increased effectiveness of the tosylate ion as a leaving group in the Menshutkin reaction. Calculated number-average molar mass values of ~6500 were found for the PV ditosylates, comparable to those found for the PV dibromides.<sup>13</sup>

Spectroscopic data were consistent with the expected PV structures. The lyotropic behavior of the PVs was investigated using polarized light microscopy and this is discussed later when porosity effects are considered.

All the polyviologens were incorporated successfully into hybrids using an experimental method similar to those described previously.<sup>13</sup> The precise choice of experimental conditions was governed by the nature of the PV and the mass fraction to be incorporated in the hybrid. Ethanol and methanol were used for experiments with TEOS and TMOS, respectively, to avoid the complication of transesterification reactions occurring. Up to 75% by mass PHV–OTs could be incorporated into the silica hybrids while retaining optical transparency, indicating that any phase separation exists on a submicrometer level, perhaps suggesting that many of these hybrids are true nanocomposites. Gels times

varied from ~2 h up to 50 h, but no obvious trends were apparent from the data reported here and a mass of other data collected in the course of the research. In particular, although in some cases the gel time was longer at higher pH, the trend was not consistent. Previous studies on TEOS using hydrochloric acid as the catalyst showed a maximum in gel time below pH 2.<sup>24</sup>

**Porosity of Silica–Polyviologen Hybrids.** The surface areas and pore-size distributions were investigated for a variety of silica–PV hybrids. The surface analysis results for these materials are shown in Table 4.

It is known that a number of factors can affect the surface area, pore volume, porosity, and pore sizes of silica xerogels.<sup>5,11,25–29</sup> Such factors include the synthetic conditions<sup>25–27</sup> (e.g., monomer concentration, *r* value, temperature, and the acidity/basicity of the catalyst) and the addition and nature (e.g., cationic, nonionic or anionic) of organic molecules and polymers.<sup>5,11,28,29</sup>

(24) Coltrain, B. K.; Melpolder, S. M.; Salva, J. M. In *Proc. IV<sup>th</sup> Int. Conf. Ultrastructure Processing of Ceramics, Glasses & Composites*; Uhlmann, D. R., Ulrich, D. R., Eds.; Wiley: New York, 1989.

(25) Chul Ro, J.; Jae Chung, I. *J. Non-Cryst. Solids* **1991**, *130*, 8.

(26) Chen, K. C.; Tsuchiya, T.; Mackenzie, J. D. *J. Non-Cryst. Solids* **1986**, *81*, 227.

(27) Munoz-Aguado, M.-J.; Gregorkiewitz, M. *J. Colloid Interface Sci.* **1997**, *185*, 459.

(28) Dabadie, T.; Ayrat, A.; Guizard, C.; Cot, L.; Lurin, C.; Nie, W.; Rioult, D. *J. Sol-Gel Sci. Technol.* **1995**, *4*, 107.

(29) Julbe, A.; Balzer, C.; Barthez, J. M.; Guizard, C.; Larbot, A.; Cot, L. *J. Sol-Gel Sci. Technol.* **1995**, *4*, 89.

Large differences in  $r$  value (water:alkoxide molar ratio) and monomer concentrations were required in the syntheses of the silica–polyviologen sol–gel hybrids to produce high quality, transparent products; however, all were acid-catalyzed ( $\text{pH} \leq 3$ ) using acetic acid and the temperature of the sol–gel reactions was the same for all the hybrid materials. Table 4 shows that virtually identical results are obtained for  $S_{\text{BET}}$ , pore volume, porosity and average pore size for the two sol–gel silicas prepared from TMOS, despite large differences in the value of  $r$  (2 and 30) and a difference in pH. The surface areas etc. obtained are similar to those quoted by others for acid-catalyzed sol–gel silicas.<sup>30</sup> For example a two-step catalyzed silica xerogel from TMOS had  $S_{\text{BET}} = 740 \text{ m}^2 \text{ g}^{-1}$ ,  $V_p = 0.345 \text{ cm}^3 \text{ g}^{-1}$ ,  $\phi = 0.43$  and  $D = 18 \text{ \AA}$ . It is therefore assumed that observations made about the silica–polyviologen sol–gel hybrids can be discussed in the context of the effects of the incorporation of the polyviologen within the silica matrix.

The presence of polyviologen had a significant effect on the BET surface area, total pore volume and porosity of the sol–gel material. The concentration, the type of polyviologen incorporated, and whether a lyotropic polyviologen solution was used in the synthesis are factors that can influence the surface area of the material. In all cases, when polyviologen was present the surface area, pore volume and porosity of the material were reduced compared to silica samples containing no added polyviologen. This might be expected since the polyviologen will have occupied some of the pore volume within the silica. The effect was relatively small for hybrids containing “low” ( $\leq 12.6\%$  PV) concentrations of polyviologen. Above about 20% PV, the concentration effects became marked. High concentrations of polyviologen, which produced initial PV solutions which were lyotropic (see below), resulted in low surface area materials with low porosity. Thus, at low polyviologen concentrations, hybrids resulted with high surface areas and high porosities, while the hybrids had low surface areas and low porosities above a certain PV concentration ( $\sim 20\%$ ). In addition, it can be seen that in cases where use of high concentration (lyotropic) PV solutions lead to low surface area hybrids, the average pore diameters were much higher than those prepared from isotropic solutions. For example, the hybrid containing 30% PBV–OTs had an average pore diameter an order of magnitude greater than hybrids made with low (or zero) PV contents. Together with the observed low porosities in such cases, this is consistent with a material containing a relatively small number of large pores with any smaller pores entirely filled with polymer. The presence of this type of pore structure has implications for the proposed use of such materials as oxygen sensors.<sup>13</sup>

Typical adsorption–desorption isotherms for the sol–gel hybrids are shown in Figures 1 and 2 for silica ( $r = 30$ ) and the hybrid containing 12.6% PHV–OTs.

The silica sample displayed a type I isotherm (Figure 1), exhibited by microporous materials.<sup>15,16,30</sup> The isotherm showed little or no hysteresis, which is indicative of microporosity and cylindrical pore geometries. However, the PHV–OTs hybrids showed evidence of type

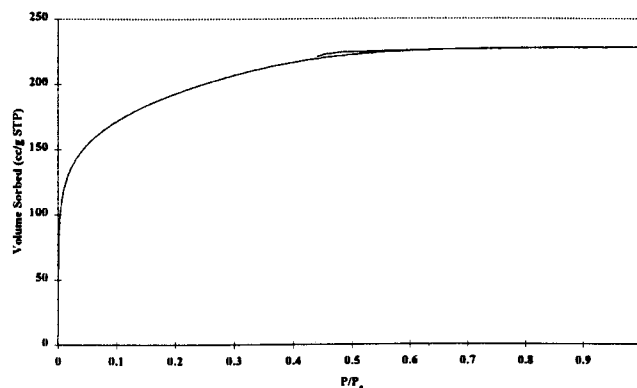


**Figure 1.** Adsorption–desorption isotherm for silica, synthesized by method 3 ( $r = 30$ ).

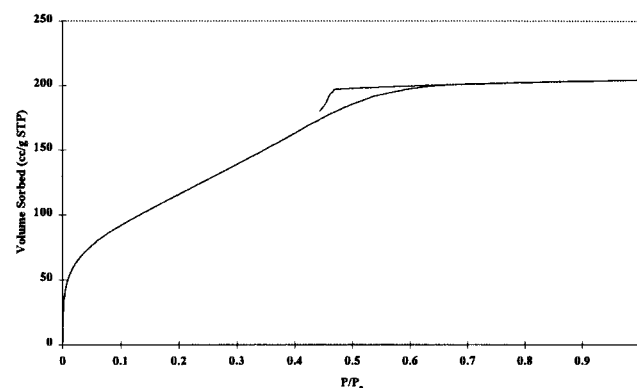


**Figure 2.** Adsorption–desorption isotherm for silica–PHV–OTs (12.6%), synthesized by method 3.

IV isotherms with type E (de Boer) hysteresis,<sup>16</sup> in which the pore geometry is “ink-bottle” shaped (in which the pore cavities are larger in diameter than the openings).<sup>15,16,30</sup> It is well-documented that acid-catalyzed silica xerogels are characterized by type I isotherms, i.e., small pores and narrow pore size distributions.<sup>25,30</sup> Additionally, base-catalyzed silica xerogels are normally associated with type IV isotherms.<sup>25,30</sup> Incorporation of polyviologen (PHV–OTs) into the silica seemed to produce hybrids exhibiting type IV isotherms under acidic conditions, indicating that the shape of the pores had been changed from smooth and cylindrical to ink-bottle shaped. Therefore, addition of polyviologen can produce hybrids not only with unusual surface fractal geometry<sup>14</sup> but can also change the pore shape.

Typical pore size distributions in the mesoporous range were calculated using the uncorrected modeless data<sup>17</sup> and are shown in Figures 3 and 4 for silica ( $r = 30$ ) and the hybrid containing 29% PHV–OTs.

The pore size distributions were very similar for silica (Figure 3) and most of the hybrid materials, with the most frequent pore diameter at  $\sim 20 \text{ \AA}$ , followed by a gradual decrease in pore volume with increasing pore radius. For the hybrid containing 29% PHV–OTs, however, the most frequent pore diameter was  $\sim 90 \text{ \AA}$  (Figure 4), although the reasons for this are unclear.

Using the Harkins–Jura equation (eq 1), the micropore surface areas and volumes of the silica–polyviologen hybrids were determined. These results are shown in Table 5, which tabulates only those materials which displayed microporosity. The micropore analysis method<sup>19</sup> was used to produce micropore size distribu-

(30) Brinker, C. J.; Scherer, G. W. *The Physics and Chemistry of Sol–Gel Processing*; Academic Press: San Diego, 1990.

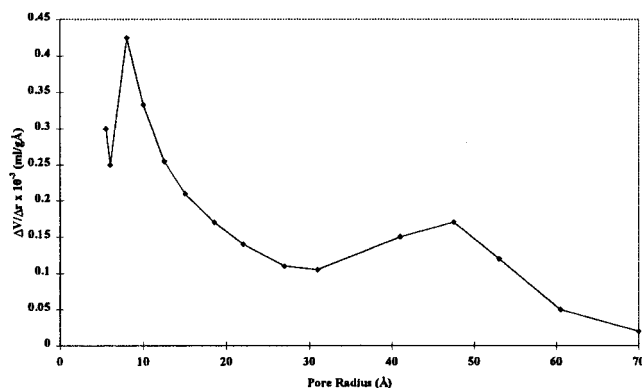


**Figure 3.** Pore volume distribution curve for silica from TMOS, synthesized by method 3 ( $r = 30$ ).

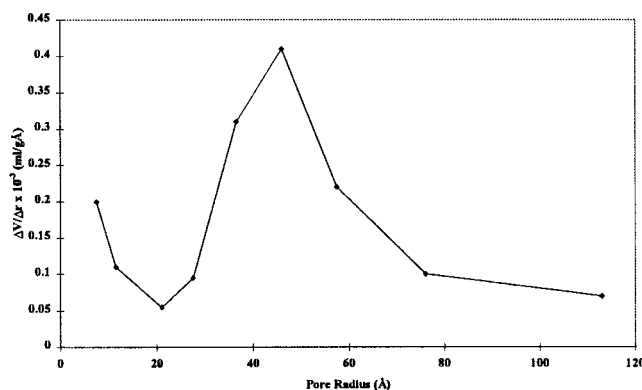


**Figure 4.** Pore volume distribution curve for silica-PHV-OTs (29%), synthesized by method 3.

**Table 5. Micropore Surface Areas and Volumes for a Variety of Sol-Gel Materials**

PV used <sup>a</sup>	% PV <sup>b</sup>	micropore surface area <sup>c</sup> /m <sup>2</sup> g <sup>-1</sup>	micropore volume <sup>d</sup> /cm <sup>3</sup> g <sup>-1</sup>
silica ( $r = 2$ )	0	315	0.134
silica ( $r = 30$ )	0	242	0.101
silica ( $r = 30$ ) <sup>e</sup>	0	38.3	0.015
PBV-Br	1	205	0.087
PBV-Br <sup>e</sup>	1	61.3	0.025
PBV-Br <sup>e</sup>	10	28.5	0.0084
PBV-Br <sup>e</sup>	20	28.4	0.011
PXV-Br	10.5	179	0.074
PBV-OTs <sup>e</sup>	37	48.5	0.017
PHV-OTs <sup>e</sup>	29	14.2	0.0031
PHV-OTs <sup>e</sup>	49	13.9	0.0014

<sup>a</sup> See Table 3 for synthetic method. <sup>b</sup> PV = polyviologen. <sup>c</sup> Equations 3 and 4. <sup>d</sup> Equation 2. <sup>e</sup> Calcined at 650 °C for 24 h.

tions. With very low concentrations of polyviologen the hybrids retained the microporosity associated with the nonhybrid materials. As the amount of polyviologen was increased, the micropore surface areas and pore volumes decreased, until in some cases there were no micropores present at all, thus producing essentially mesoporous materials.

Micropore size distributions were calculated using the MP analysis method<sup>19</sup> for the sol-gel materials described in Table 5. From the micropore distribution, the most frequent pore diameter for silica from TMOS ( $r = 30$ ) was  $\sim 11$  Å, with the distribution being bimodal. The silica from TMOS ( $r = 2$ ) had a similar micropore distribution to the  $r = 30$  silica. The addition of polyviologen resulted in distributions displaying the most frequent pore diameter in the range 9–13 Å in

those cases where the hybrids displayed microporosity. The bimodal distributions observed for the neat silicas closely resemble the distributions previously measured for two silica-methyl viologen (MV) gels<sup>31</sup> and a microporous silica gel,<sup>19</sup> although for the former gels only the micropores were studied. The silica-MV gels (both containing  $\sim 5\%$  MV) both gave type I isotherms indicative of microporous materials. One sample had a BET surface area of 81.17 m<sup>2</sup> g<sup>-1</sup> and a total pore volume of 0.0607 cm<sup>3</sup> g<sup>-1</sup> (78.1% microporosity), whereas the other had a BET surface area of 148.1 m<sup>2</sup> g<sup>-1</sup> and a total pore volume of 0.1347 cm<sup>3</sup> g<sup>-1</sup> (70.7% microporosity). In contrast, the silica-polyviologen hybrids were not primarily microporous materials, although microporosities were highest for low PV contents.

Incorporation of polyviologen within a sol-gel silica matrix clearly has an effect on the structure of the silica network in terms of the BET surface area, pore volume and the porosity, although the effects are complex.

**Porosity of Silica Prepared by Calcination of Silica-PV hybrids.** A number of the sol-gel samples were calcined at 650 °C for 24 h and their surface area analysis results are shown in Table 6.

Upon calcination of amorphous inorganic oxide materials prepared by the sol-gel route, there is generally a decrease in the BET surface area, total pore volume, and porosity, due to aging and consequent network reorganization caused by the thermal treatment of the sol-gel material.<sup>32</sup> The use of organic templates can help to overcome this, although thermal restructuring of the oxide network can still result in a pore structure very different to the original "footprint" of the template molecule.<sup>4,9</sup> At low PV contents, thermal treatment led to a reduction in the overall porosity and specific surface area of the material; however, at high PV content, there was an increase in the surface area and porosity upon calcination. In these cases, removal of the polyviologen had a greater effect on the pore structure than aging alone, resulting in the "emptying" of pores otherwise filled with the encapsulated polyviologen. For example, in the case of the sol-gel hybrid containing 20% PBV-Br, the surface area increased from 1.02 to 162 m<sup>2</sup> g<sup>-1</sup> upon calcination, the porosity increased by a factor of over 50 and the average pore size was reduced. This final observation is consistent with the formation of a much higher proportion of small pores, but says nothing about the fate of the original large pores. The PHV-OTs systems, in particular, lead to formation of silica products with high mesoporosities and high surface areas in comparison to the neat silica samples. The removal of the organic component during calcination was confirmed by elemental analysis (Table 7). As expected, calculated values for carbon, hydrogen, and nitrogen content were zero or close to zero in all cases. The small but significant carbon content observed for PHV-OTs (12.6%) was probably a result of some carbonation of the PV, since all the hydrogen and nitrogen had been eliminated successfully.

Typical adsorption-desorption isotherms for the calcined systems are shown in Figures 5 and 6 for silica ( $r = 30$ ) and the hybrid containing 12.6% PHV-OTs.

(31) Dai, S.; Sigman, M. E.; Burch, E. L. *Chem. Mater.* **1995**, *7*, 2054.

(32) Hench, L. L.; West, J. K. *Chem. Rev.* **1990**, *90*, 33.

Table 6. Surface Analysis of Calcined Sol–Gel Materials

PV used <sup>a</sup>	% PV <sup>b</sup>	BET surface area/m <sup>2</sup> g <sup>-1</sup>	C value	total pore volume (V <sub>p</sub> )/cm <sup>3</sup> g <sup>-1</sup>	porosity (φ) <sup>d</sup> /%	average pore diameter (D) <sup>e</sup> /Å
silica ( <i>r</i> = 30)	0	212	134	0.105	19	17.8
PBV–Br	1	241	172	0.128	22	15.5
PBV–Br	10	314	93.3	0.177	28	20.3
PBV–Br <sup>f</sup>	20	162	122	0.088	16	19.6
PBV–OTs <sup>f</sup>	37	118	109	0.056	11	17.1
PHV–OTs <sup>f</sup>	12.6	486	77.6	0.317	41	23.5
PHV–OTs <sup>f</sup>	29	260	93.1	0.168	27	23.2
PHV–OTs <sup>f</sup>	49	346	86.1	0.226	33	23.5
PHV–OTs <sup>f</sup>	75	393	70.2	0.379	45	34.7

<sup>a</sup> See Table 3 for synthetic method. <sup>b</sup> PV = polyviologen. <sup>c</sup> At  $P/P_0 = 0.9907$ . <sup>d</sup> Porosity,  $\phi = V_p/(V_p + 0.455)(100\%)$ . <sup>e</sup> Average pore diameter,  $D = 0.9(4V_p/A)$ ;  $A$  is the BET specific surface area. <sup>f</sup> Synthesized from a lyotropic solution of polyviologen.

Table 7. Elemental Analysis of Calcined Silica–Polyviologen Sol–Gel Hybrids

hybrid	elemental analysis (found)/mass%
neat silica ( <i>r</i> = 30)	C, 0.07; H, 0.0; N, 0.0
	C, 0.05; H, 0.0; N, 0.0
PHV–OTs (12.6%)	C, 0.68; H, 0.0; N, 0.0
	C, 0.60; H, 0.0; N, 0.0
PHV–OTs (29%)	C, 0.00; H, 0.0; N, 0.0
	C, 0.00; H, 0.0; N, 0.0
PBV–Br (10%)	C, 0.00; H, 0.0; N, 0.0
	C, 0.00; H, 0.0; N, 0.0

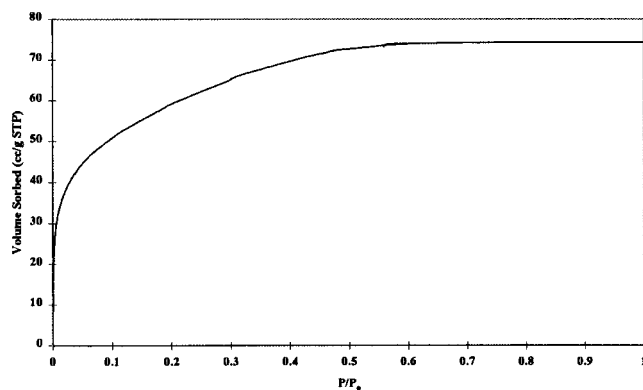


Figure 5. Adsorption–desorption isotherm for silica, synthesized by method 3 (*r* = 30), and then calcined at 650 °C for 24 h.

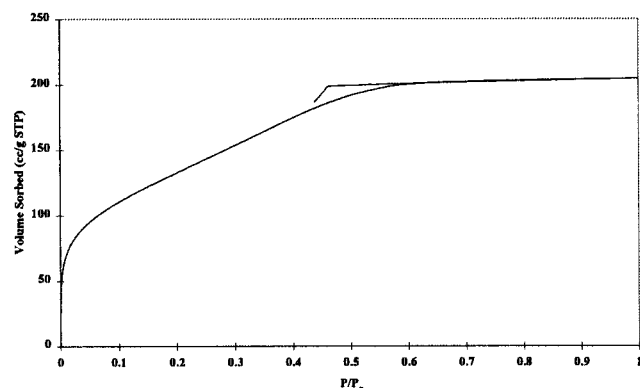


Figure 6. Adsorption–desorption isotherm for silica–PHV–OTs (12.6%), synthesized by method 3, and then calcined.

Calcination had little or no effect on the isotherms (cf. Figures 3 and 4), suggesting that the pore geometries remained the same after thermal treatment. Although the pore shapes remained the same, the surface area, porosity, total pore volume and the average pore size could be manipulated by the addition of polyviologen and thermal treatment. For example, the most frequent

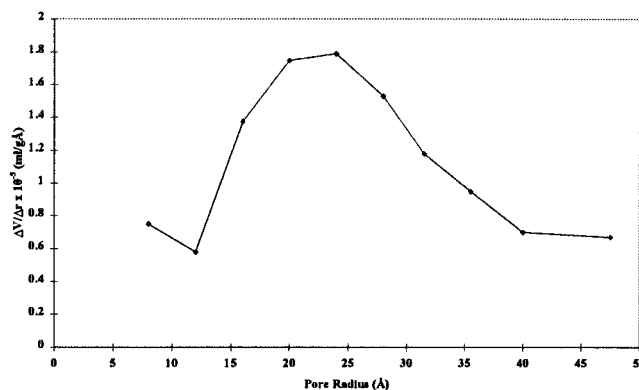


Figure 7. Pore volume distribution curve for silica from TMOS, synthesized by method 3 (*r* = 30), and then calcined.

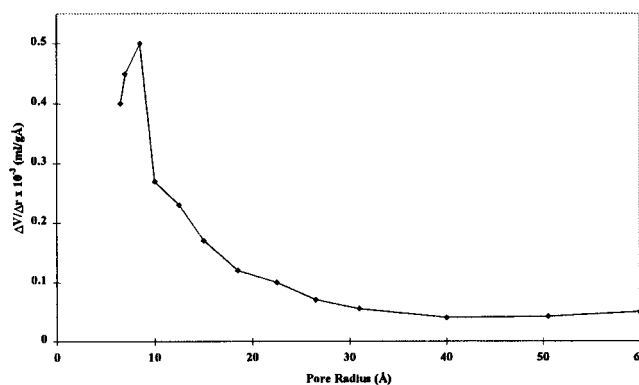
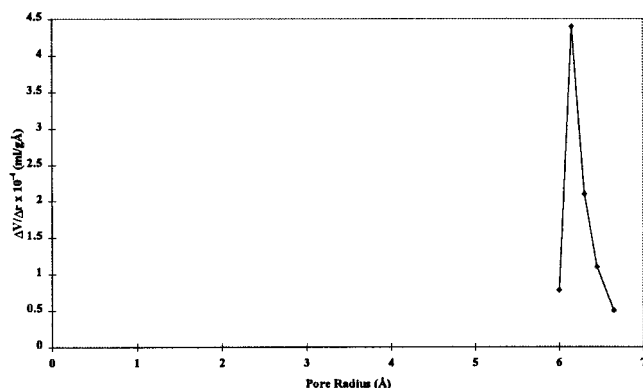


Figure 8. Pore volume distribution curve for silica–PHV–OTs (29%), synthesized by method 3, and then calcined.

pore diameter for silica from TMOS (*r* = 30) increased upon calcination by over a factor of 2 to 44 Å (Figure 7), in agreement with the observations of Chul Ro et al.<sup>25</sup> who found that above 500 °C, the surface area of an acid-catalyzed silica gel decreased and the pore size increased.

For the calcined hybrid samples, mean pore diameters of ~20 Å or slightly greater were normally observed, suggesting that the mesopore size distribution curves were relatively unchanged upon calcination, although the shapes of the distributions sometimes differed from those of silica. The hybrid containing 12.6% PBV–OTs fitted this general trend. Conversely, for the hybrid containing 29% PHV–OTs the most frequent pore diameter of ~90 Å was dramatically reduced to 18 Å upon calcination (Figure 8). In this case, there was also a narrowing of the pore size distribution upon calcination.



**Figure 9.** Micropore volume distribution for silica-PBV-Br (10%), synthesized by method 1, and then calcined.

In cases where the as-synthesized products contained micropores, the micropore surface areas and volumes were reduced upon calcination (Table 5), due to the aging effect of the thermal treatment.<sup>32</sup> Additionally, the calcined hybrids had lower micropore surface areas and volumes than the calcined silica containing no added polyviologen; however, other silica-polyviologen hybrids without micropores before calcination displayed microporosity after calcination—the presence of micropores following calcination is surprising since at the temperature of calcination (650 °C) a complete collapse of any micropores might be expected.<sup>25,32</sup> In these cases, the encapsulated polyviologen either protected the micropores from collapse upon calcination or some filled mesopores rearranged to micropores on calcination. Nonetheless, in those cases, micropore surface areas and micropore volumes were still low compared to overall surface areas and pore volumes. An interesting result is that for the silica-PHV-OTs hybrid (12.6%), which contained no micropores and retained this lack of microporosity even after calcination. This material was mesoporous and the pore geometry had been changed from smooth and cylindrical to ink-bottle. It is possible that any micropores had been filled by the encapsulated polyviologen and that upon calcination the polyviologen was removed and the micropores were destroyed. The absence of micropores may also have resulted from the polyviologen (a concentration and/or polyelectrolyte effect) influencing the growth of the silica network, thus resulting in a material which was mesoporous even upon removal of the polyviologen. Incorporation of polyviologen within a sol-gel silica matrix clearly had an effect on the growth of the silica network in terms of the BET surface area, pore volume, and the porosity, although the effects are complex.

From the micropore size distribution, the most frequent pore diameter for silica from TMOS ( $r = 30$ ) remained virtually unchanged ( $\sim 12$  Å) after calcination, but the initial bimodal distribution was replaced by a broad distribution. Calcination also caused a large decrease in pore volume ( $\Delta V/\Delta r$ ). After calcination of the hybrids, the most frequent pore diameter and  $\Delta V/\Delta r$  both decreased. Micropore size distributions for the calcined hybrids which showed no initial microporosity were variable. Calcined silica-PBV-Br (10%), for example, showed a very narrow distribution (Figure 9), while the corresponding 20% PV system showed a bimodal distribution (Figure 10), although the total microporosity was low in both cases.

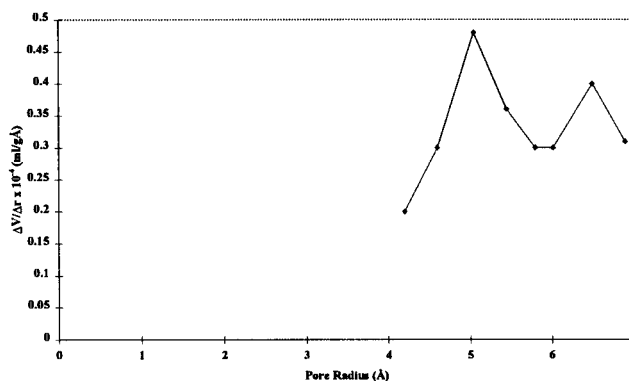


**Figure 10.** Micropore volume distribution for silica-PBV-Br (20%), synthesized by method 2, and then calcined.

Sato et al.<sup>11</sup> studied the pore size distribution of calcined sol-gel silica gels (acid-catalyzed then base-catalyzed TEOS) prepared using the cationic polymer quaternized polyethylene imine (PEI). It was observed that the more PEI added (up to 16.5 wt %) the greater the shift toward mesoporosity, which was attributed to electrostatic interactions between the silica sol particles and the polyions. A similar shift has been noticed for the silica-polyviologen hybrids although not as large as for PEI. Saegusa<sup>33</sup> synthesized porous silica gels by calcination of poly(2-methyl-2-oxazoline)/silica (from TEOS) sol-gel hybrids. Depending on the feed ratio (polymer:TEOS) surface areas ranged from 114 to 810 m<sup>2</sup> g<sup>-1</sup>, and the pore volumes ranged from 0.073 to 0.504 cm<sup>3</sup> g<sup>-1</sup>. The average pore diameters ranged from 20 to 40 Å, comparable to those found for the silica-polyviologen hybrids.

**Development of Structure in Silica-Polviologen Hybrids.** The above results show that it was possible to prepare amorphous silica materials, which were largely or entirely mesoporous, through the incorporation of polyviologens and their removal by elevated temperature calcination. The results of this study and previous work<sup>14</sup> suggest that the presence of the PV affects the structure of the forming silica network, resulting in control of the final silica pore structure. Of particular interest are systems based on PHV-OTs, where silica of high surface area (up to  $\sim 500$  m<sup>2</sup> g<sup>-1</sup>) and high mesoporosity (pores  $>98\%$  meso) could be obtained after calcination of the initial hybrid. These polymers can produce lyotropic mesophases in solution at concentrations typical of those used in the sol-gel reaction. The use of supramolecular assemblies of liquid crystalline (LC) structures derived from block copolymers and cationic surfactants to template structure in growing silica networks has been reported by a number of workers in recent years, including the groups of Attard,<sup>34,35</sup> Guizard,<sup>5,28,36</sup> Göltner,<sup>37</sup> and Marignan.<sup>38</sup> Impressive control of final product morphology has been

(33) Saegusa, T. *J. Macromol. Sci.-Chem.* **1991**, A28, 817.

(34) Attard, G. S.; Glyde, J. C.; Göltner, C. G. *Nature* **1995**, 378, 366.

(35) Attard, G. S.; Edgar, M.; Göltner, C. G. *Acta Mater.* **1998**, 46, 751.

(36) Guizard, C. G.; Julbe, A. C.; Ayrat, A. *J. Mater. Chem.* **1999**, 9, 55.

(37) Göltner, C. G.; Henke, S.; Weissenberger, M. C.; Antonietti, M. *Angew. Chem., Int. Ed. Engl.* **1998**, 37, 613.

(38) Porcar, L.; Marignan, J.; Gulik-Krzywicki, T. *J. Sol-Gel. Sci. Technol.* **1998**, 13, 99.



observed in these cases. Lyotropic behavior in polyviologens has been studied extensively by Bhowmik and Han<sup>39–44</sup> who observed lyotropism for a range of PVs in different solvents above a critical concentration which was dependent on the nature of the PV and the anion. Above a certain concentration, aqueous or methanolic solutions of many of the PVs used in this study showed strong shear birefringence and textures expected of lyotropic materials when studied by polarized light microscopy (PLM). SAXS studies on the silica–PV hybrids showed that in systems based on initially lyotropic PV solutions, the silica structure developed in a different way to materials made from initially isotropic PV solutions.<sup>14</sup> Evidence here also seemed to suggest that in some cases (such as the PHV–OTs systems), use of lyotropic PV solutions led to silica pore structures which were different to those obtained from isotropic PV solutions or in the absence of added polymer.<sup>45</sup> It is doubtful, however, whether these effects arose simply from the lyotropic behavior of the PV since further PLM studies have shown that the mesophases are destroyed in the complex sol–gel solution (e.g., TMOS, water, methanol, acetic acid), which agrees with the findings of others.<sup>28,34,35</sup> It is not clear whether the mesophases re-form during the sol–gel transformation or whether reaction conditions can be found to allow mesophases to persist in these systems (e.g., by continuous removal of byproduct alcohol<sup>34,35</sup>)—these will be the subject of future work.

The differences in porosity and fractal geometry observed in some of these systems are most likely to arise from some combination of the following factors: (1) the type of polyviologen, e.g. number of linking methylene units, nature of anion; (2) the concentration of polyviologen; (3) electrostatic interactions; and (4) hydrophobic hydration effects (cf. those postulated in zeolite synthesis<sup>1–3</sup>).

Both 3 and 4 are in part dependent on 1 and 2. Electrostatic interactions between the cationic nitrogens of the PV and the silanol oxygen atoms in the growing silica network can be envisaged as shown in Figure 11. Such interactions are likely to be more marked at high PV concentration and may also depend on the counterion. The involvement of lyotropic mesophases cannot

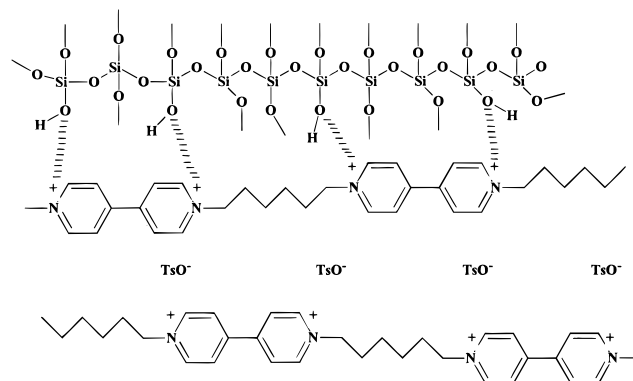


**Figure 11.** Possible electrostatic interactions between N<sup>+</sup> and Si–OH groups.

be completely eliminated, however, and even if LC supramolecular assemblies do not act as morphological templates in these systems, their presence could influence the degree of electrostatic interaction within the system.

### Conclusions

The pore structure of silica–polyviologen hybrids prepared by the hydrolytic sol–gel route has been probed by nitrogen adsorption–desorption experiments. The presence of the polymer had a significant effect on the porosity of both the hybrids and the silica products obtained by calcination of the hybrids. The results showed a dependence of porosity on concentration of the PV which, together with earlier results,<sup>14</sup> suggest that the PV is affecting the structure of the forming silica network. The nature of this effect is interesting since these polymers offer the possibility of both topological (through lyotropic mesophases) and functional (cationic nitrogens) control of the inorganic oxide synthesis. The present results do not allow a lyotropic mechanism to be proven, but electrostatic interactions between the organic and inorganic phases seem likely to influence the structures formed. Further work will be aimed at determining whether PV mesophases can be maintained throughout the sol–gel transformation and their effect on the structure of the products. To the best of our knowledge, there have been no reports to date of the use of cationic polymeric mesophases for the control of silica structure in the sol–gel reaction. Future work will also look in more detail at the evolution of silica porosity from the hybrids, including the possibility of removing the polymers in a controlled way by chemical means.<sup>9</sup>

**Acknowledgment.** The UK Engineering and Physical Sciences Research Council (EPSRC) is thanked for the award of a studentship to M.J.A. Elemental analyses were carried out by Ms. N. Walker.

CM991129E

(39) Han, H. S.; Bhowmik, P. K. *TRIP* **1995**, *3*, 199.

(40) Bhowmik, P. K.; Han, H. S. *J. Polym. Sci., Polym. Chem. Ed.* **1995**, *33*, 1745.

(41) Han, H.; Bhowmik, P. K. *ACS Polym. Prepr.* **1995**, *36*, 328.

(42) Han, H.; Bhowmik, P. K. *ACS Polym. Prepr.* **1995**, *36*, 330.

(43) Bhowmik, P. K.; Akhter, S.; Han, H. *J. Polym. Sci., Polym. Chem. Ed.* **1995**, *33*, 1927.

(44) Bhowmik, P. K.; Xu, W.; Han, H. S. *J. Polym. Sci., Polym. Chem. Ed.* **1994**, *32*, 3205.

(45) It should be noted that no evidence has been found for crystallinity in these systems using X-ray diffraction and wide-angle X-ray scattering.<sup>14</sup> In addition, no useful information on morphology could be obtained by electron microscopy.